



HAL
open science

Non-gaussian effects in the cage dynamics of polymers

Alistar Ottochian, Cristiano de Michele, Dino Leporini

► **To cite this version:**

Alistar Ottochian, Cristiano de Michele, Dino Leporini. Non-gaussian effects in the cage dynamics of polymers. *Philosophical Magazine*, 2008, 88 (33-35), pp.4057-4062. 10.1080/14786430802348060 . hal-00513945

HAL Id: hal-00513945

<https://hal.science/hal-00513945>

Submitted on 1 Sep 2010

HAL is a multi-disciplinary open access archive for the deposit and dissemination of scientific research documents, whether they are published or not. The documents may come from teaching and research institutions in France or abroad, or from public or private research centers.

L'archive ouverte pluridisciplinaire **HAL**, est destinée au dépôt et à la diffusion de documents scientifiques de niveau recherche, publiés ou non, émanant des établissements d'enseignement et de recherche français ou étrangers, des laboratoires publics ou privés.



Non-gaussian effects in the cage dynamics of polymers

Journal:	<i>Philosophical Magazine & Philosophical Magazine Letters</i>
Manuscript ID:	TPHM-08-May-0160
Journal Selection:	Philosophical Magazine
Date Submitted by the Author:	15-May-2008
Complete List of Authors:	Ottochian, Alistar; Università di Pisa, Fisica De Michele, Cristiano; University of Roma, Fisica Leporini, Dino; University of Pisa, Fisica
Keywords:	glass transition, molecular dynamic simulations, polymers
Keywords (user supplied):	glass transition, molecular dynamic simulations, polymers
<p>Note: The following files were submitted by the author for peer review, but cannot be converted to PDF. You must view these files (e.g. movies) online.</p> <p>paperTPHM-08-May-0160.tex</p>	



Philosophical Magazine
Vol. 00, No. 00, 00 Month 200x, 1–8

RESEARCH ARTICLE

Non-gaussian effects in the cage dynamics of polymers

A. OTTOCHIAN^{†*}, C. DE MICHELE^{‡§} and D. LEPORINI^{†‡}

[†]*Dipartimento di Fisica "Enrico Fermi", Università di Pisa, Largo B. Pontecorvo 3,
I-56127 Pisa, Italy;*

[‡]*INFM-CRS Soft*

[§]*Dipartimento di Fisica, Università di Roma "La Sapienza" Piazzale Aldo Moro, 2,
00185 Roma, Italy*

(Received 00 Month 200x; final version received 00 Month 200x)

The correlation between the fast cage dynamics and the structural relaxation is investigated in a model polymer system. It is shown that the cage vibration amplitude, as expressed by the Debye-Waller factor (DW), and the relaxation time τ_α collapse on a single universal curve with a simple analytic form when the temperature, the density, the chain length and the monomer-monomer interaction potential are changed. For the physical states with the same τ_α the coincidence of the mean-square displacement, the intermediate scattering function and the non-gaussian parameter is observed in a wide time window spanning from the ballistic regime to the onset of the Rouse dynamics driven by the chain connectivity. The role of the non-gaussian effects is discussed.

Keywords: glass transition; polymers dynamics; Molecular Dynamics simulation

1. Introduction

There is a growing interest in the relation between the fast vibrational dynamics and the long-time structural relaxation occurring in viscous systems and supercooled liquids close to their glass transition [1–20]. This resulted in studies of the vibrational dynamics of both glasses [6, 13–17] and fluid systems [9, 12, 20].

Recently, the universal correlation between the amplitude of the caged dynamics, as expressed by the Debye-Waller factor (DW), and the structural relaxation time τ_α has been evidenced by simulations and experiments on several physical systems including molecular liquids, polymers and metallic alloys in a wide range of fragility [20]. It was found that the shape of the related scaling function is also controlled by the non-gaussianity of the kinetic unit displacement [20]. The present paper presents new numerical results to provides further insight on the actual weight of non-gaussian effects.

2. Theory

The glass transition has been pictured as the freezing of a liquid in an Aperiodic Crystal Structure (ACS) where the viscous flow is due to activated jumps over

*Corresponding author. Email: ottochian@df.unipi.it

energy barriers $\Delta E \propto k_B T a^2 / \langle u^2 \rangle$ where a is the displacement to overcome the barrier and $\langle u^2 \rangle$ is the DW factor of the liquid, i.e. the amplitude of the rattling motion within the cage of the nearest neighbours atoms [3]. The ACS picture leads to the Hall-Wolynes (HW) equation, $\tau_\alpha, \eta \propto \exp(a^2/2\langle u^2 \rangle)$, a relation which has been derived by others too [5, 12, 21]. The HW equation relies on the condition that τ_α exceeds the vibrational time scales. When the HW equation is compared with the experiments, one notes strong deviations from the predicted linear dependence between $\log \tau_\alpha$ and $1/\langle u^2 \rangle$ [12]. To generalize the HW equation, one considers a distribution $p(a^2)$ of the square displacement to overcome the energy barriers [20]. Following the central limit theorem, the gaussian form is adopted, $p(a^2) = \mathcal{N} \cdot \exp[-(a^2 - \overline{a^2})^2/2\sigma_{a^2}^2]$ where \mathcal{N} is the normalization constant, $\overline{a^2}$ and σ_{a^2} are the average and the standard deviation respectively. Note that, since $\Delta E \propto a^2$, this choice corresponds to a gaussian distribution of energy barriers. The distribution is taken to be independent of the state parameters because the average displacement of the kinetic unit within τ_α is weakly dependent on τ_α [22]. In contrast, the DW factor depends on the state parameters [7, 8]. If one averages the HW expression over $p(a^2)$, one obtains the following generalized HW expression (GHW):

$$\tau_\alpha = \tau_0 \exp \left(\frac{\overline{a^2}}{2\langle u^2 \rangle} + \frac{\sigma_{a^2}^2}{8\langle u^2 \rangle^2} \right). \quad (1)$$

Eq. 1 neglects the very weak DW-dependence of τ_0 . If the linear temperature dependence of the DW factor is assumed, GHW reduces to other results reported for supercooled liquids [23], polymers [24] or models of glassy relaxation [25, 26].

3. Model

A coarse-grained model of a linear freely-jointed polymer is used. Non-bonded monomers interact via a generalized Lennard-Jones pair potential $U_{p,q}(r)$ with $U_{p,q}(r) = \epsilon(q-p)^{-1}[p(\sigma^*/r)^q - q(\sigma^*/r)^p] + U_{cut}$ with $\sigma^* = 2^{1/6}\sigma$. The parameters p and q control the stiffness of the attractive and the repulsive part, respectively. All quantities are in reduced units: length in units of σ , temperature in units of ϵ/k_B , and time in units of $\sigma\sqrt{m/\epsilon}$, where m and k_B are the monomer mass and the Boltzmann constant, respectively. The energy unit is given by the depth of the potential well ϵ . We also set $m = k_B = 1$. The potential is cut and shifted to zero by U_{cut} at $r = 2.5$. The potential $U_{p,q}(r)$ reduces to the usual Lennard-Jones (LJ) potential by setting $p = 6, q = 12$. Bonded monomers interact with a potential which is the sum of the FENE (Finitely Extendible Nonlinear Elastic) potential and the LJ potential (see ref. [20] for further details). This results in a bond length $b = 0.97$. Samples with $N \simeq 2000$ monomers were used. Equilibration runs were performed in isothermal-isobaric (NPT) or canonical (NTV) ensembles. Data were collected under microcanonical conditions by integrating the equations of motion with a reversible multiple time steps algorithm, i.e. the r-RESPA algorithm [27]. Physical states with different values of the temperature T , the density ρ , the chain length M and the monomer-monomer interaction potential $U_{p,q}(r)$ were studied. See ref. [20] for further details.

1
2
3
4
5
6
7
8
9
10
11
12
13
14
15
16
17
18
19
20
21
22
23
24
25
26
27
28
29
30
31
32
33
34
35
36
37
38
39
40
41
42
43
44
45
46
47
48
49
50
51
52
53
54
55
56
57
58
59
60

4. Results and discussion

In this section the translational dynamics and the relaxation of the monomeric unit are studied. Changing the state parameters (M, ρ, T, q, p) results in changes of both the DW factor and the relaxation time τ_α . It was found that, when different physical states have the same relaxation time, both their translational dynamics, as expressed by the mean square displacement (MSD), and their relaxation, as expressed by the self part of the intermediate scattering function (ISF), are coincident from the ballistic regime up to the onset of the connectivity effects (Rouse regime) at times fairly longer than τ_α [20]. The resulting clusters of curves are shown in Fig.1 for both MSD ($\langle r^2(t) \rangle = N^{-1} \sum_1^N \langle (\mathbf{r}_i(t) - \mathbf{r}_i(0))^2 \rangle$) and ISF ($F_s(q_{max}, t) = N^{-1} \sum_1^N \langle \exp[i\mathbf{q}_{max} \cdot (\mathbf{r}_i(t) - \mathbf{r}_i(0))] \rangle$), q_{max} refers to the maximum of the static structure factor). ‘[Insert figure 1 about here]’ Fig.1 also shows the definition of τ_α via the equation $F_s(q_{max}, \tau_\alpha) = 1/e$. The existence of clusters of physical states with similar dynamics over the wide time range from the vibrational regime to the long-time relaxation suggests that the latter are correlated. To investigate this issue, it was noted that the location of the inflection point of the MSD does not depend on the state point, i.e. it always occurs at the same time $t = t^*$ in the log-log plot of MSD [20]. This gives the opportunity of a clear-cut definition of the DW factor as $\langle u^2 \rangle \equiv \langle r^2(t^*) \rangle$. The plot of τ_α vs $\langle u^2 \rangle$ leads to a master curve for the numerical results well described by the GHW Eq.1 which fits the experimental results over about eighteen orders of magnitude [20].

We investigated if, in addition to MSD and ISF, other quantities exhibit identical time-dependence when evaluated for the clusters of states with identical τ_α values shown in Fig.1. The results for the non-gaussian parameter (NGF) $\alpha_2(t) = (3\langle r^4(t) \rangle) / 5\langle r^2(t) \rangle^2 - 1$, which quantifies the dynamical heterogeneity of the system at a given time t [28], are shown in Fig.2. ‘[Insert figure 2 about here]’ NGF vanishes if the monomer displacement is a gaussian process. Fig.2 shows that NGF increases between the end of the ballistic regime ($t \sim 0.1$) and roughly τ_α . In principle there are no reasons to infer from ISF and MSD any particular behaviours of other quantities depending by moments of displacement distribution, e.g. such as NGF. Despite this we account that physical states with coincident MSD and ISF (see Fig.1) have equal NGF up to about τ_α too. For longer times the NGF of physical states with equal τ_α but different chain length differ also due to the onset of connectivity effects (Rouse regime) [29, 30].

It has been already shown that the magnitude of the non-gaussian parameter is related to the curvature of the GHW Eq.1 when the plot $\log \tau_\alpha$ vs $\langle u^2 \rangle^{-1}$ is considered [20]. Indeed, the ratio of the quadratic and the linear terms of Eq.1 with respect to $\langle u^2 \rangle^{-1}$, $\mathcal{R} \equiv \sigma_{a_2}^2 / (4a^2 \langle u^2 \rangle)$ increases with the height of NGF α_{2max} and, if the latter vanishes, \mathcal{R} does the same [20]. The inset of Fig.2 shows the increase of α_{2max} by increasing τ_α . If the non-gaussian effects are missing, ISF reduces to $F_s^g(q_{max}, t) = \exp(-\frac{1}{6}q_{max}^2 \langle r^2 \rangle)$. The first correction to $F_s^g(q, t)$ due to the non-gaussian effects depends on NGF and reads [31] :

$$\bar{F}_s(q, t) = \exp\left(-\frac{1}{6}q^2 \langle r^2 \rangle\right) \left[1 + \frac{1}{2}\alpha_2(t) \left(\frac{1}{6}q^2 \langle r^2 \rangle\right) + \mathcal{O}\left(\left(\frac{1}{6}q^2 \langle r^2 \rangle\right)^2\right) \right]. \quad (2)$$

‘[Insert figure 3 about here]’ Fig.3 compares the numerical results for ISF with the approximation $\bar{F}_s(q_{max}, t)$. It is seen that, when $\tau_\alpha \gtrsim 10^2$, $\bar{F}_s(q_{max}, t)$ poorly approximates the numerical results, thus showing that the non-gaussian effects on the relaxation are not accounted for by the first correction to $F_s^g(q_{max}, t)$, i.e. they are

not small. Thanks to Fig.3 we can state that non-gaussian terms became critically determinant to describe structural relaxation approaching GT, in particular high orders moments of displacement distribution increase. However, in spite of the large deviations of $\overline{F}_s(q_{max}, t)$ from the exact results, the inset of Fig.3 shows that the relative error between τ_α and the approximated estimate $\overline{\tau}_\alpha$ (to be defined by the equation $\overline{F}_s(q_{max}, \overline{\tau}_\alpha) = 1/e$) is reasonable.

5. Conclusions

The correlations between the fast dynamics of the monomers within the cage of the first neighbours and the long-time structural relaxation are studied. It is shown that physical states with equal τ_α exhibit coincident MSD, ISF and NGF from the ballistic regime up to the onset of the connectivity effects (Rouse regime) at times fairly longer than τ_α . The first correction to the gaussian approximation of ISF disagrees from the numerical results for $\tau_\alpha \gtrsim 10^2$ because high orders moments of displacement distribution critically increase. However, the relative error between τ_α and the approximated estimate $\overline{\tau}_\alpha$ stays within reasonable bounds.

Acknowledgment

Discussions with Dr. Luca Larini are acknowledged. Computational resources by "Laboratorio per il Calcolo Scientifico" (Physics Department, University of Pisa), financial support from MUR within the PRIN project "Aging, fluctuation and response in out-of-equilibrium glassy systems" and FIRB project "Nanopack" are acknowledged.

References

- [1] C.A. Angell, *Science* 267 (1995) p.1924.
- [2] J. Shao and C.A. Angell, *Proc. XVIIth International Congress on Glass, Beijing*, 1 (1995) p.311.
- [3] R.W. Hall and P.G. Wolynes, *J. Chem. Phys.* 86 (1987) p.2943.
- [4] J.C. Dyre, N.B. Olsen, and T. Christensen, *Phys. Rev. B* 53 (1996) p.2171.
- [5] J.C. Dyre and N.B. Olsen, *Phys. Rev. E* 69 (2004) p.042501.
- [6] L.M. Martinez and C.A. Angell, *Nature* 410 (2001) p.663.
- [7] K.L. Ngai, *J. Non-Cryst. Solids* 275 (2000) p.7.
- [8] K.L. Ngai, *Phil. Mag.* 84 (2004) p.1341.
- [9] F. Starr et al., *Phys. Rev. Lett.* 89 (2002) p.125501.
- [10] P. Bordat et al., *Phys. Rev. Lett.* 93 (2004) p.105502.
- [11] A. Widmer-Cooper and P. Harrowell, *Phys. Rev. Lett.* 96 (2006) p.185701.
- [12] U. Buchenau and R. Zorn, *Europhys. Lett.* 18 (1992) p.523.
- [13] T. Scopigno et al., *Science* 3 (2003) p.849.
- [14] A.P. Sokolov et al., *Phys. Rev. Lett.* 7 (1993) p.2062.
- [15] U. Buchenau and A. Wischniewski, *Phys. Rev. B* 70 (2004) p.092201.
- [16] V.N. Novikov and A.P. Sokolov, *Nature* 431 (2004) p.961.
- [17] V.N. Novikov, Y. Ding and A.P. Sokolov, *Phys.Rev.E* 71 (2005) p.061501.
- [18] S.N. Yannopoulos and G.P. Johari, *Nature* 442 (2006) p.E7.
- [19] J.C. Dyre, *Rev. Mod. Phys.* 78 (2006) p.953.
- [20] L. Larini et al., *Nature Physics* 4 (2008) p.42.
- [21] V.N. Novikov and A.P. Sokolov, *Phys. Rev. E* 67 (2003) p.031507.
- [22] C.A. Angell, *J.Non-Crystalline Sol.* 131-133 (1991) p.13-p.31.
- [23] H. Bässler, *Phys. Rev. Lett.* 58 (1987) p.767.
- [24] J.D. Ferry, L.D.J. Grandine, and E.R. Fitzgerald, *J. Appl. Phys.* 24 (1953) p.911.
- [25] C. Monthus and J.P. Bouchaud, *J. Phys. A: Math. Gen.* 29 (1996) p.3847.
- [26] J.P. Garrhan and D. Chandler, *Proc. Natl. Acad. Sci.* 100 (2003) p.9710.
- [27] M.E. Tuckerman and B.J. Berne, *J. Chem. Phys.* 95 (1991) p.8362.
- [28] S.C. Glotzer and M. Vogel, *Phys. Rev. E* 70 (2004) p.061504.
- [29] G.D. Smith et al., *J. Chem. Phys.* 114 (2001) p.4285.
- [30] W. Paul, *Chem. Phys.* 284 (2002) p.59.
- [31] B.R.A. Nijboer and A. Rahman, *Physica* 32 (1966) p.415.

1
2
3
4
5
6
7
8
9
10
11
12
13
14
15
16
17
18
19
20
21
22
23
24
25
26
27
28
29
30
31
32
33
34
35
36
37
38
39
40
41
42
43
44
45
46
47
48
49
50
51
52
53
54
55
56
57
58
59
60

Figure 1. (a) MSD time-dependence in the selected cases (M, ρ, T, q, p) : set A $[(2, 1.086, 0.7, 7, 6), (3, 1.086, 0.7, 7, 6), (10, 1.086, 0.7, 7, 6), (10, 1.033, 0.7, 8, 6)]$, set B $[(2, 1.033, 0.6, 10, 6), (3, 1.039, 0.7, 11, 6), (3, 1.041, 0.7, 11, 6)]$, set C $[(2, 1.033, 0.5, 10, 6), (3, 1.056, 0.7, 12, 6), (5, 1.033, 0.6, 12, 6), (10, 1.056, 0.7, 12, 6)]$, set D $[(3, 1.086, 0.7, 12, 6), (5, 1.086, 0.7, 12, 6), (10, 1.086, 0.7, 12, 6)]$ and set E $[(2, 1.0, 0.7, 12, 11)]$. The MSDs are multiplied by indicated factors. (b) corresponding ISF curves. Four sets of clustered curves (A through D) show that, if states have equal τ_α (marked with star on each curve), the MSD and ISF curves coincide from times fairly longer than τ_α down to the crossover to the ballistic regime at least. Adapted from ref.[20].

Figure 2. Time-dependence of the the non-gaussian parameter (NGF) for the same states listed in caption of Fig.1. The stars denote the time $t = \tau_\alpha$. The plot shows that for states with equal τ_α not only MSD and ISF coincide between t^* and τ_α (see Fig.1) but also NGF does the same within the statistical uncertainty. The inset shows the increase of the maximum of NGF with τ_α . The dashed line is a parabolic guide for the eyes.

Figure 3. Comparison between the numerical ISF (continuous lines) of Fig.1 and the first correction to the gaussian approximation $\bar{F}_s(q_{max}, t)$ (dashed lines). The inset shows the relative error between τ_α and the estimate $\bar{\tau}_\alpha$, as drawn from $\bar{F}_s(q_{max}, \bar{\tau}_\alpha) = 1/e$. Selected cases (M, ρ, T, q, p) : set A $[(2, 1.086, 0.7, 7, 6)]$, set B $[(2, 1.033, 0.6, 10, 6)]$, set C $[(2, 1.033, 0.5, 10, 6)]$, set D $[(2, 1.033, 0.5, 10, 6), (3, 1.056, 0.7, 12, 6), (5, 1.033, 0.6, 12, 6), (10, 1.056, 0.7, 12, 6)]$, set D $[(3, 1.086, 0.7, 12, 6)]$ and set E $[(2, 1.0, 0.7, 12, 11)]$.

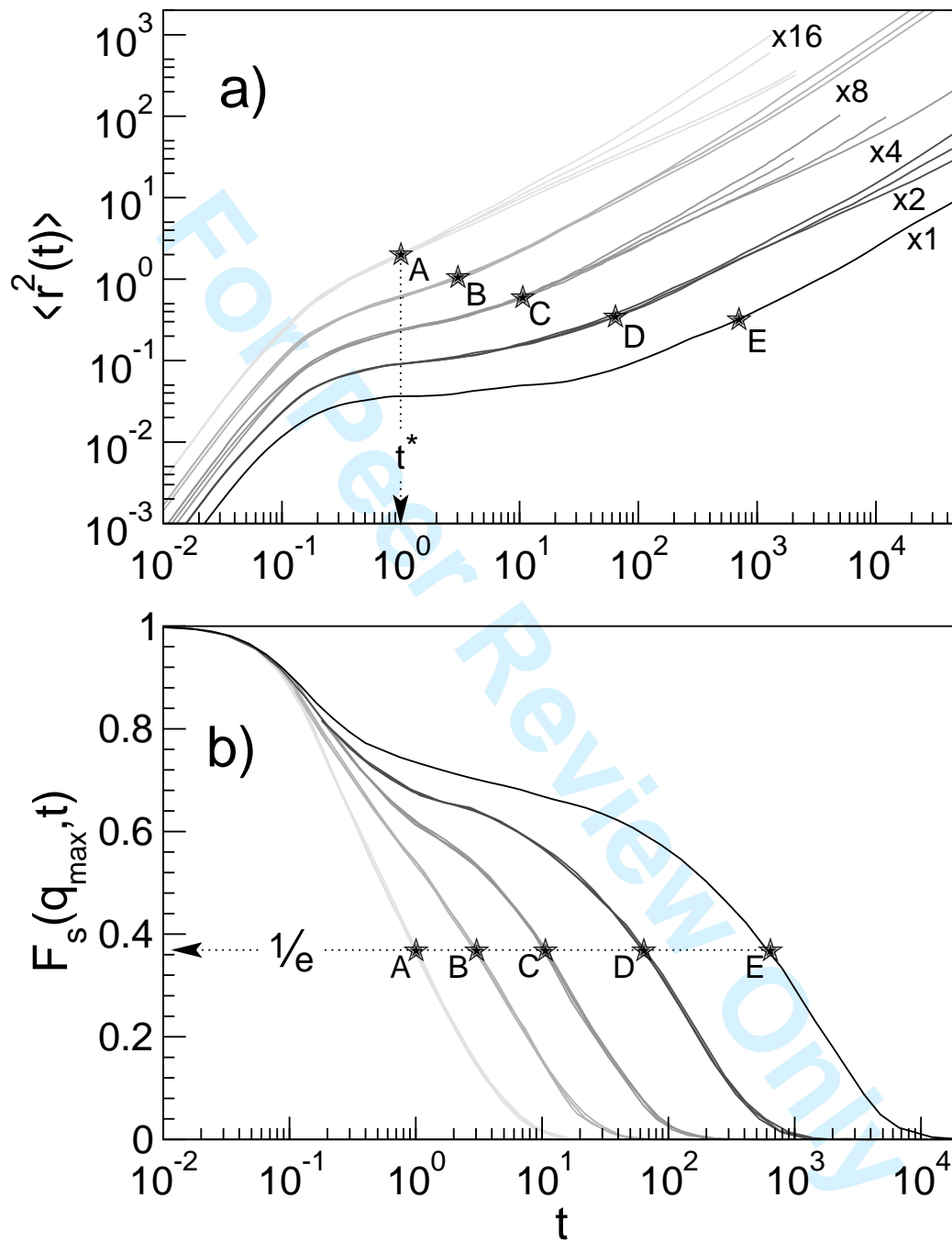


FIGURE 1

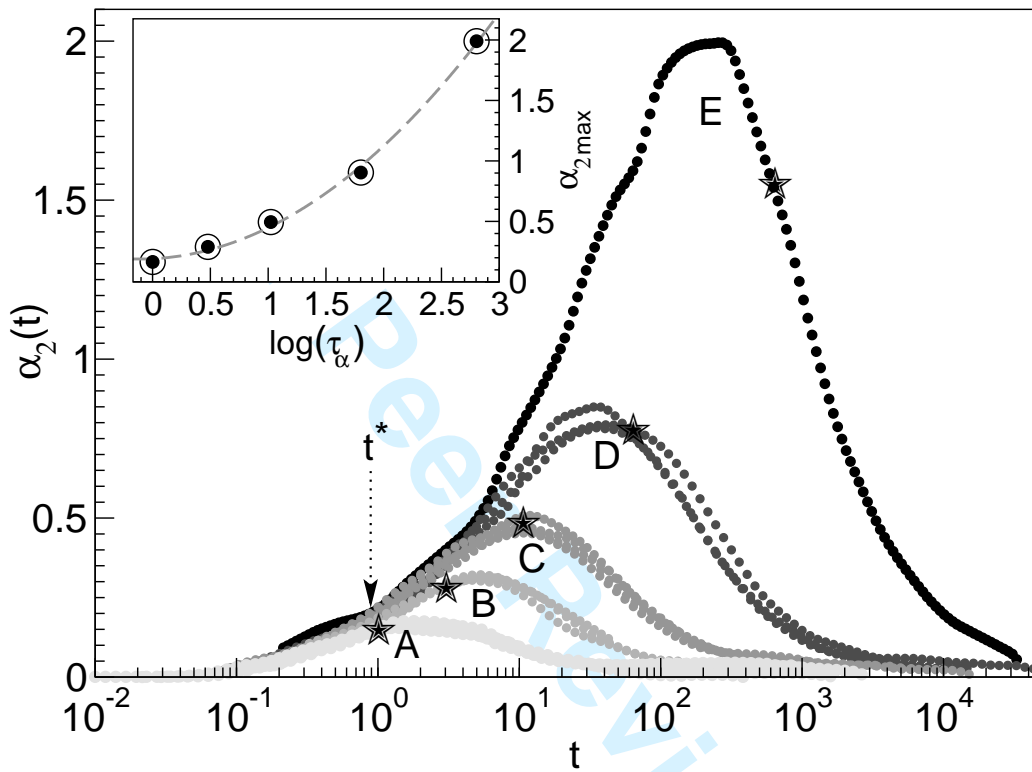


FIGURE 2

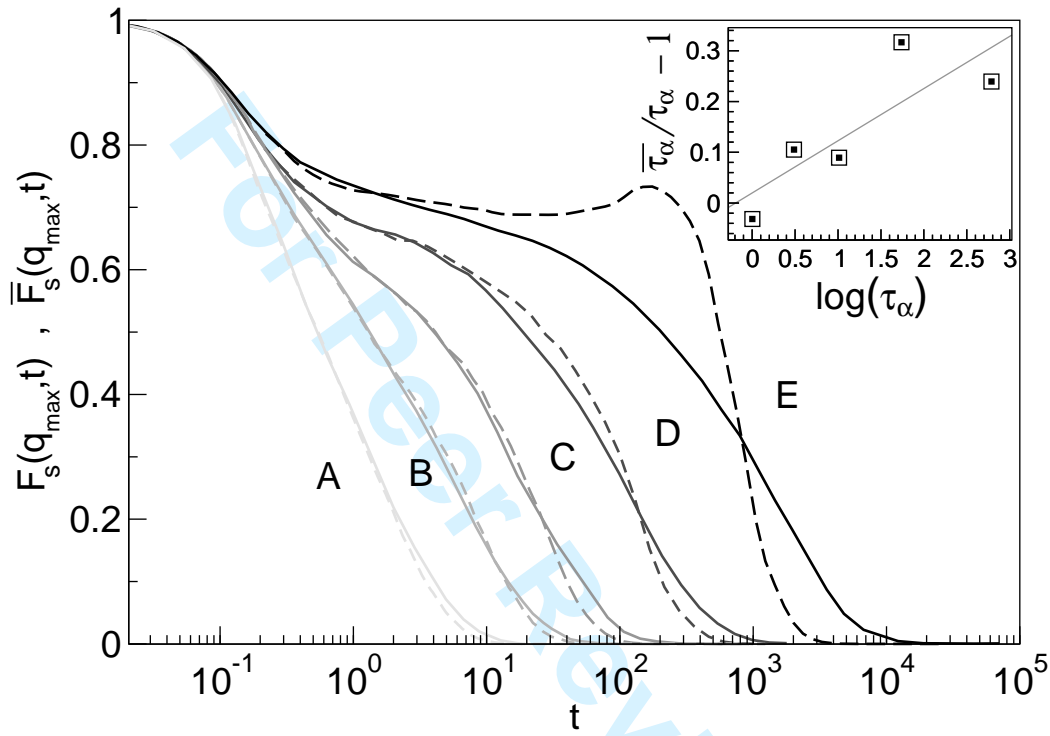
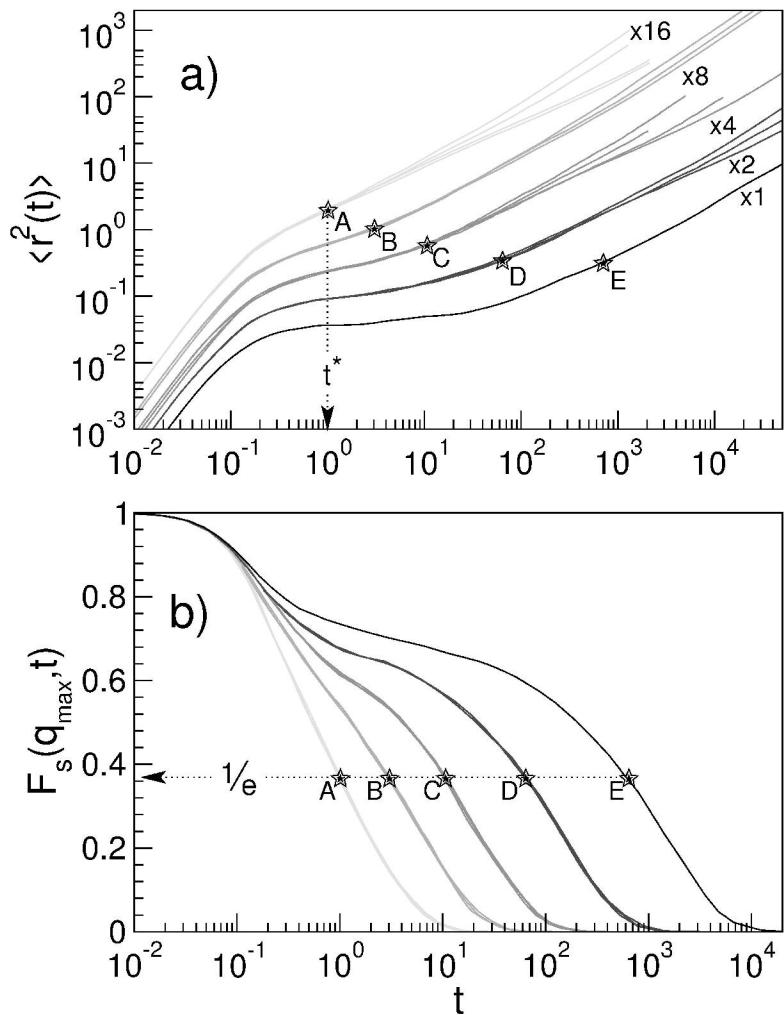


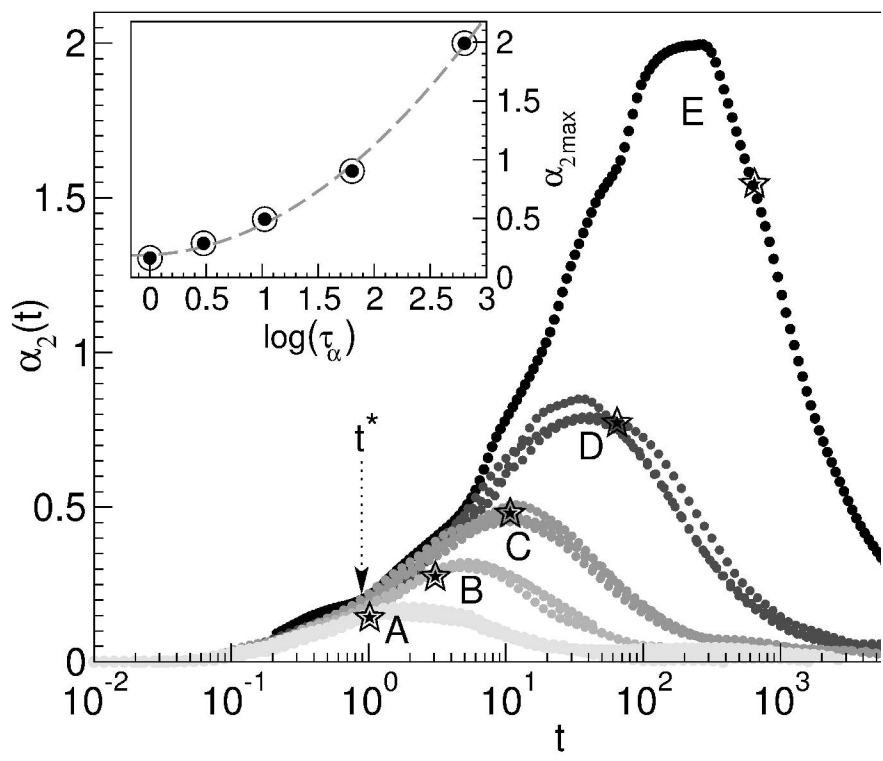
FIGURE 3

1
2
3
4
5
6
7
8
9
10
11
12
13
14
15
16
17
18
19
20
21
22
23
24
25
26
27
28
29
30
31
32
33
34
35
36
37
38
39
40
41
42
43
44
45
46
47
48
49
50
51
52
53
54
55
56
57
58
59
60



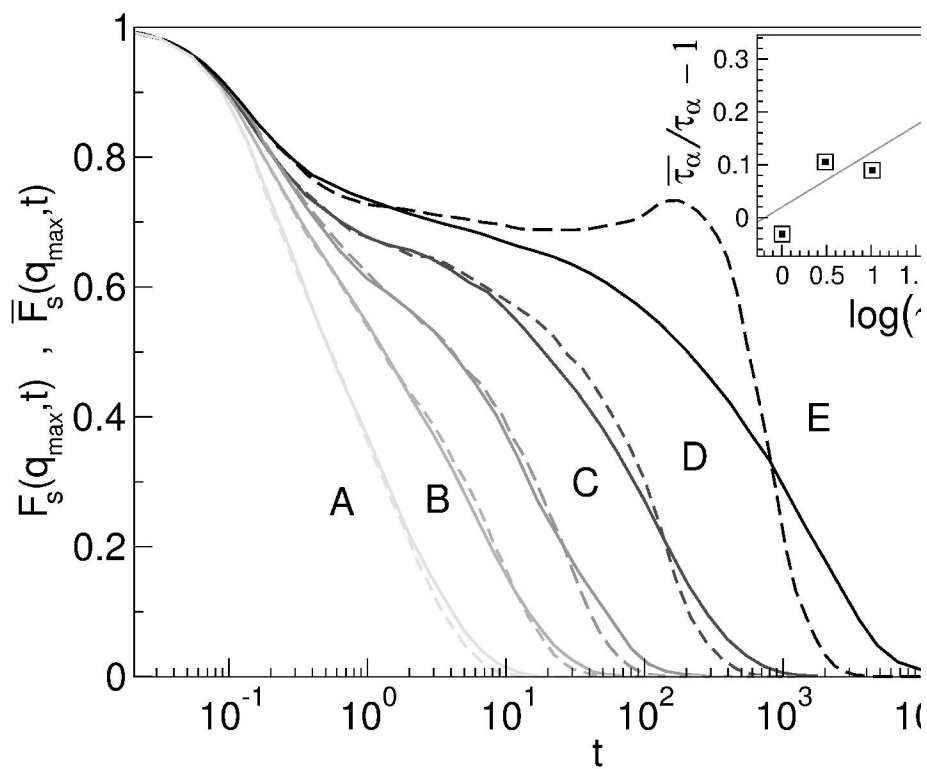
215x279mm (600 x 600 DPI)

1
2
3
4
5
6
7
8
9
10
11
12
13
14
15
16
17
18
19
20
21
22
23
24
25
26
27
28
29
30
31
32
33
34
35
36
37
38
39
40
41
42
43
44
45
46
47
48
49
50
51
52
53
54
55
56
57
58
59
60



215x279mm (600 x 600 DPI)

1
2
3
4
5
6
7
8
9
10
11
12
13
14
15
16
17
18
19
20
21
22
23
24
25
26
27
28
29
30
31
32
33
34
35
36
37
38
39
40
41
42
43
44
45
46
47
48
49
50
51
52
53
54
55
56
57
58
59
60



215x279mm (600 x 600 DPI)